Voroshilov, Pavel M.; Simovski, Constantin R.; Belov, Pavel A.; Shalin, Alexander S.

Light-trapping and antireflective coatings for amorphous Si-based thin film solar cells

Published in:
Journal of Applied Physics

DOI:
10.1063/1.4921440

Published: 01/01/2015

Document Version
Publisher's PDF, also known as Version of record

Please cite the original version:
Voroshilov, P. M., Simovski, C. R., Belov, P. A., & Shalin, A. S. (2015). Light-trapping and antireflective coatings for amorphous Si-based thin film solar cells. *Journal of Applied Physics*, *117*(20).
https://doi.org/10.1063/1.4921440

Light-trapping and antireflective coatings for amorphous Si-based thin film solar cells

Pavel M. Voroshilov, Constantin R. Simovski, Pavel A. Belov, and Alexander S. Shalin

Citation: Journal of Applied Physics **117**, 203101 (2015); doi: 10.1063/1.4921440
View online: https://doi.org/10.1063/1.4921440
View Table of Contents: http://aip.scitation.org/toc/jap/117/20
Published by the American Institute of Physics

Light-trapping and antireflective coatings for amorphous Si-based thin film solar cells

Pavel M. Voroshilov,[1,2] Constantin R. Simovski,[1,2] Pavel A. Belov,[1] and Alexander S. Shalin[1,3,4]
[1]*ITMO University, Kronverkskiy pr. 49, 197101 St. Petersburg, Russia*
[2]*Department of Radio Science and Engineering, School of Electrical Engineering, Aalto University, P.O. Box 13000, 00076 Aalto, Finland*
[3]*Ulyanovsk Branch of Kotel'nikov Institute of Radio Engineering and Electronics of Russian Academy of Sciences, Goncharov Str. 48, 432011 Ulyanovsk, Russia*
[4]*Ulyanovsk State University, L. Tolstoy-str., 42, Ulyanovsk 432017, Russia*

(Received 25 October 2014; accepted 10 May 2015; published online 22 May 2015)

In this paper, we study the efficiency of several types of all-dielectric, non-resonant, antireflection, and light-trapping coatings for the enhancement of photovoltaic absorption in thin-film silicon solar cells. We compare the enhancement of the photovoltaic absorption offered by a square array of nano-pillar shaped voids in the dielectric covering of the cell with that granted by a flat blooming layer, and a densely packed array of dielectric nanospheres. We optimize these coatings and show that the newly proposed nanostructure allows a significant increase of the photovoltaic absorption. The dependence of antireflection and light-trapping properties on the angle of incidence is numerically investigated, and it is shown that the array of voids keeps optimal also after averaging over the incidence angles. © *2015 AIP Publishing LLC*. [http://dx.doi.org/10.1063/1.4921440]

I. INTRODUCTION

Nowadays, a great attention is paid to researches in photovoltaics, which is one of the most promising trends in the modern energy industry. A large amount of toxic waste generated by the high-purity semiconductor production forces to pay special attention to thin-film solar cells (TFSCs).[1] The advantages of TFSC are the small amount of purified semiconductor required, since the thickness of the photovoltaic (PV) layer is smaller than the diffusion length of minority charge carriers, i.e., 150–300 nm (Refs. 1–3) and also the possibility of roll-to-roll processing on flexible substrates.[4] The disadvantage of TFSC is parasitic optical losses due to a small thickness of a PV layer. A solar radiation passes through a PV layer and then it is absorbed in the substrate that leads to a harmful heating. A conventional antireflection coating (ARC) is not effective in this case, since the decrease of the reflection from the surface of the solar cell results in the increase of the transmission.[2]

Many suggestions for increasing absorption in solar cells are based on the use of light-trapping structures (LTS). Such structures allow to reduce both the reflection from a solar cell and the transmission through its PV layer. It can be achieved due to the localization of high-intensity near field in the volume of a semiconductor.[5–19] Some authors offer the combination of PV layer and photonic crystals,[6,7] optically dense arrays of semiconductor protrusions,[8,9] and plasmonic nanostructures.[10–18] Some plasmonic LTS performed as nanotextured semiconductor coatings convert the incident plane wave into waveguide modes propagating along the PV layer as in an optical waveguide.[16–18] The ability of textured coatings to convert light over the entire spectral range, in which a solar cell operates is limited by a small thickness of PV layer, making texturing inefficient for unijunction TFSC with the thickness of PV layer about 150–300 nm. However, this restriction known as Yablonovich limit[20,21,23] is derived strictly in the frame of geometrical optics approximation and valid only when this approach is applicable to describe the interaction of light with a rough surface, i.e., for the transmissive phase grating.[21,23] It can be overcome by replacing protrusions on the surface of the semiconductor by the grid of plasmonic nanoelements,[16–18] in which an incident plane wave excites surface plasmon polaritons due to the Wood's diffraction anomalies.[22] Under the condition of phase synchronism of surface plasmon polaritons with the guided modes of PV layer, it is possible to achieve a fairly effective concentration of energy of an incident wave in the PV layer of the thickness of 300–400 nm (Refs. 16 and 18) and even of 200 nm.[17,23] The disadvantages of such light-trapping structures are unavoidable scattering losses of waveguide modes in the elements of a grid, an inability to convert 100% of an incident light into waveguide modes in the PV layer, and also complexity and high cost of the implementation of required plasmonic arrays.[15–19,23]

Most papers on plasmonic LTS are based on the increase of the PV absorption in the spectral range of plasmon resonances of nanoelements (silver or gold nanoparticles).[10–13] From the microscopic point of view, this increase occurs due to the fact that plasmon nanoparticles enhance the electric field locally that leads to the formation of the so-called "hot spots"—regions with the subwavelength light concentration. Since hot spots arise in the region occupied by the metal particles and by the doped semiconductor, the light is effectively absorbed in them, so the reflection from the surface of TFSC and transmission through the PV layer are significantly reduced. These structures are called plasmonic absorbers and may be divided into two classes. The first class of PA is

random arrays of nanoparticles grown by chemical means. In these structures, only averaged parameters such as average size of the particles and their surface density can be optimized.[10–13] The optical properties of irregular arrays can be adequately described by a model of the effective medium with the complex dielectric constant experiencing a Lorentz-type resonance with a relatively small magnitude and broad band in the visible range.[13] The main drawbacks of such absorbers are losses in metal elements (large at high concentrations of plasmonic elements) and scattering (significant at low concentrations of plasmonic elements).

The second class of plasmonic absorbers is represented by regular grids of plasmonic nanoparticles of different shapes with optimized geometry of the unit cell.[14–17,23] Such nanoparticles refer to receiving nanoantennas (NA) because they efficiently transform the incidence plane wave into a set of hot spots. Typically, these NA have several narrow band plasmon resonances that correspond to the resonant excitation of multipoles in them.[15,16] Note that other structures besides arrayed metal NA can be used as LTS. Dielectric cavity resonators can also work as NA due to the coupling with the substrate.[24] The advantage of properly designed NA is the possibility to localize the hot spot outside its volume. So the solar energy dissipation in such NA (and therefore its harmful heating) is much smaller than in the case of random plasmonic absorbers producing hot spots partially inside nanoparticles.

Nevertheless, the arrays of NA are expensive structures and they do not provide an ideal solution. Though it is possible to almost eliminate losses in the metal,[25,26] still the effect of NA keeps resonant, and even a multiresonance NA increases the absorption in a PV layer in a relatively narrow wavelength band. In works 25 and 26, the band enhanced by NA covers nearly one half of the operation band of TFSC and grants the PV absorption 30% higher than an ARC. However, this result corresponds to very small thicknesses d of the PV layers—in these works, one emphasized on either organic or CIGS-based TFSC with $d = 60–150$ nm. For silicon-based TFSC, the optimal thickness of the PV layer is $d = 300–500$ nm. Inspecting the literature on these TFSC, we have not found evidences of their significant enhancement by metal NA. The enhancement is claimed in many papers, however, only for thinner layers which are impractical for generation purposes (see, e.g., in work 14).

In recent papers, one can find LTS performed as arrays of densely packed dielectric nanospheres.[24,28–31] These structures operate as an effectively continuous anti-reflecting coating in a rather broad wavelength range and simultaneously possess light-trapping properties. The effect of LTS appears in structures studied in Refs. 24 and 28–31 due to the resonant photonic nanojet regime, due to whispering gallery modes excited at several wavelengths and due to photonic crystal trapping that arises for the oblique incidence. The all-dielectric design solution is attractive for practice since the mass production costs can be minimized using the self-organization of such arrays.[28] However, the light-trapping effect for such arrays is still resonant, i.e., intrinsically narrow-band. In our work 32, we suggested to slightly increase these spherical particles. Though this increase slightly magnifies the scattering losses, it allows the mechanism of broadband light focusing into the PV layer. This opens new possibilities in the light trapping. We have shown that slightly submicron polystyrene spheres on top of a PV layer of thickness 300 nm allow the reduction of both reflection and transmission losses. In our other works, we suggested a broadband antireflection coating—an array of nano-voids in the dielectric covering.[29–31] It was shown that such a nanostructured layer can be optimized for any particular PV materials by changing the size of voids. Meanwhile, the spectral range of the reflection damping is broader than that achievable for a standard homogeneous ARC, such as silica or silicon nitride.

It becomes interesting to compare novel structures—the LTS based on polystyrene spheres and the ARC on nano-voids. Their impact is reasonable to normalize to the case of a standard blooming layer. Really, flat antireflection coatings represent currently the major and most common way to improve the efficiency of all solar cells, even TFSC. Therefore, study of the impact of nanostructures on the efficiency of solar cells would be incomplete without an appropriate comparison with a flat ARC. In this paper, we consider all three nanostructures and show that, to our surprise, the structure of arrayed nano-voids may possess light-trapping properties, which make it the most advantageous for both normal and oblique incidences of solar light.

II. THE MAIN CONCEPT OF NON-RESONANT ALL-DIELECTRIC COATINGS FOR ABSORPTION ENHANCEMENT IN TFSC

Let us consider the system, depicted in Fig. 1 and representing three types of all-dielectric coatings under study. The first type is a layer of mutually touching polystyrene spheres (we show a unit cell in Fig. 1(a)). In our previous work,[32] it was shown that this structure possesses light-trapping properties in the visible range for the case when the diameter of the sphere is close to 1 μm due to the non-resonant focusing effect. A layer of closely packed micron or submicron spheres is placed on top of the aluminum-doped zinc oxide (AZO) transparent electrode (AZO layer has thickness 200 nm), and a 300-nm thick layer of a-Si (10-nm thick p-layer, 280 nm i-layer, and 10 nm n-layer) is sandwiched between this electrode and the bottom electrode of AZO that in our model is assumed to be semi-infinite. Though it can be practically as thin as few μm, the incident light does not penetrate into a mechanical carrier (bulk substrate) due to strong PV absorption and nonzero optical decay in AZO. The density of minority charge carriers in all doped parts is equal to 3×10^{18} cm^{-3}, Ref. 33. This TFSC may be prepared using the atomic layer deposition with quantum efficiency up to 70%, whereas nanospheres can be grown using the self-organization of colloids or simply mechanically applied using the centrifuge. The optical constants of materials were taken from Refs. 34–36.

The second structure is the ARC shown in Fig. 1(b) is based on nano-voids shaped as cylinders or truncated cones in the dielectric covering.[29–31] The broadband anti-reflecting operation is achieved due to the variation of the effective optical thickness of such structure versus the wavelength.[29]

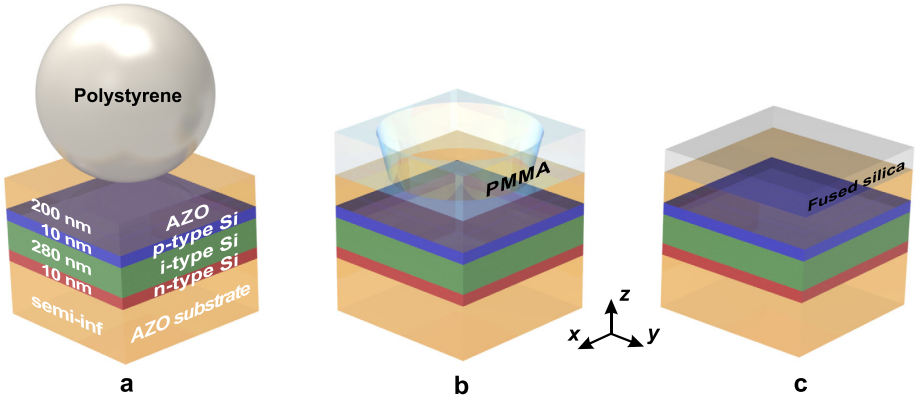

FIG. 1. Schematic views of thin film solar cell with three types of all-dielectric coatings for TFSC: a close-packed layer of dielectric (polystyrene) nano- or microspheres (a), a square array of tapered nano-voids in the superstrate (b), and a homogeneous film ARC (c). All these structures are deposited on the aluminum-doped zinc oxide (AZO) layer (thickness 200 nm) with 10 nm p-type, 280 nm i-type, 10 nm n-type amorphous silicon layers and semi-infinite AZO substrate under it.

In contrast, a homogeneous blooming film, depicted in Fig. 1(c), can totally suppress the reflection only at a single wavelength, for which the blooming resonance holds, and therefore its operational band is rather narrow.

Obviously, two effects allow the enhancement of the PV absorption due to any LTS or ARC. The first effect is suppression of the reflection from the structure, and the second one is the suppression of parasitic transmission of light through the PV layer. To fulfill the first condition, the LTS should operate as an ARC, while the second effect requires the field concentration in the PV layer so that the absorption would be higher than the plane-wave decay. It is obvious that this mechanism cannot be realized by using a homogeneous flat film, however, it is allowed for our 2d structure. For both 1st and 2d structures, the suppression of reflection occurs mostly due to the dipole polarization of inclusions.[29–31] The localization of radiation may arise due to the high-order Floquet harmonics, which correspond to multipole moments of higher orders excited in a unit cell.[37] The impact of this collection of multipoles in our work 32 was described very simply—as the collimation of the transmitted light by individual spheres. The deal between two useful effects gives an optimal operation. The main question of this paper—is such an optimum possible for voids, which were previously considered as an ARC? If the structure with voids possesses light-trapping properties, it may be more advantageous than the LTS of sphere since it is mechanically robust.

III. NORMAL INCIDENCE OF LIGHT

A. Absorption enhancement

First of all, let us note that the considered thin film solar cell is the cell with homogeneous photocurrent, because both upper and lower contacts are flat AZO films. The inhomogeneous behavior of current in vertical direction could take place if the contacts are grid-like (because the current is directed vertically not everywhere) or in the case of bulk solar cells (because of the diffusion). The interrelation between optical absorption and photocurrent was investigated in details, e.g., in Ref. 38 and it was shown that for solar cells with homogeneous photocurrent the generation of electron-hole pairs (and, correspondingly, photocurrent itself) depends on the absorption linearly. Therefore, the optical absorption increasing leads to the photocurrent rising, so in this paper we will speak about optical absorption only.

Let us consider the case of normal incidence of light on the structures under consideration, as well as determine the optimal parameters of nanospheres and nano-voids for the achievement of the highest values of the PV absorption in semiconductor layers. In Ref. 32, we applied numerical-analytical method for this optimization problem. Approximate ranges of parameters of nanostructures corresponding to optimal antireflective and light-trapping properties were determined analytically in the frame of this method. Further, we optimized structures by the brute force method in Comsol Multiphysics and CST Microwave Studio. The details of the analytical method are given in Ref. 32.

First, let us optimize the flat ARC for the system under consideration. The transfer matrix method gave us the following result: best parameters of ARC are the following: $d = 94$ nm thickness and refractive index $n = 1.36$. In this case, the absorption enhancement in comparison with non-coated TFSC is about

$$A_{\text{pure}}^{\text{ARC}} = \frac{\int A_{\text{ARC}}\, d\nu}{\int A_{\text{pure}}\, d\nu} = 1.062, \tag{1}$$

where A_{pure}, A_{ARC}—absorption in the i-layer of a-Si for pure TFSC and for TFSC with a flat ARC, respectively. It is necessary to mention that the most common ARC for silicon-based TFSC, covered with AZO layer, is a film of fused silica glass. Taking into account the dispersion of fused silica,[39] we found that for the optimal thickness $d = 85$ nm the absorption enhancement is equal 4.6%, which is not so different from the optimal 6.2% resulting from Eq. (1). Extended calculations using the well-known exact formulas for the fields in a multilayer structure allow us to assert that there is no flat blooming layer (even with high refractive indices non-achievable for natural transparent media) that would improve the efficiency of our TFSC more than by 6.2%. This is so because the pure TFSC is also a multilayer designed so that its reflectance is quite small over the visible range. The numerical optimization of ARC with help of Comsol Multiphysics fits analytical calculations very well and gives the same result.

Let us now consider the dependence of the integral absorption in the operating range of TFSC on the parameters of the nanostructures located on the surface of TFSC. The ratio of the integral absorption calculated in the presence of a layer of closely packed spheres (A_{spheres}) to the value A_{ARC} corresponding to an optimal flat ARC–$A_{\text{ARC}}^{\text{spheres}}$ is shown in Fig. 2(a). It is clear that the PV absorption is higher compared to the case of the flat ARC for the range of the sphere radius 190–290 nm. The optimal radius is equal to 250 nm, then the integral absorption enhancement is 3.7% compared to the ARC (and 8.5% with respect to the case of pure solar cell).

In the case of nano-voids, the number of parameters to be optimized is greater, that makes the task difficult but more promising. We have optimized the depth, radius, taper angle, and the distance between the adjacent holes. Fig. 2(b) shows the plot analogous to that shown in Fig. 2(a), but for several values of the depth. We show only the dependencies corresponding to the optimal value of the distance between adjacent voids (30 nm) and to the optimal angle (10°) to avoid cluttering. These optimal values were obtained from the optimization of the structure by numerical methods. The presence of a small taper angle turns out to be an advantage. Namely, slightly tapered voids can be obtained using the nanoimprint lithography and namely such voids are optimal.

As it can be seen from Fig. 2(b), the highest PV absorption holds for the depth of voids $d = 300$ nm and the radius of voids $r = 180$ nm. The enhancement of the absorption is $(A_{\text{ARC}}^{\text{void}} - 1) \cdot 100 = 5.6\%$ compared to the flat ARC and $(A_{\text{pure}}^{\text{void}} - 1) \cdot 100 = 10.5\%$ compared to the pure surface of our TFSC. Thus, the proposed coating, which is an array of nano-voids in the layer of PMMA, located on TFSC, is slightly more efficient than the ordered layer of nanospheres. PV absorption spectra for the system with different coatings are shown in Fig. 3. As can be seen from Fig. 3, the PV absorption is quite small at long wavelengths, and the presence of any coating does not substantially affect its value due to pretty low optical absorption of a-Si in the range of 650–800 nm. On the other hand, in accord to Fig. 3 the integral absorption of the pure TFSC is equal 42%, which is quite high value for a TFSC. At 500–550 nm, the spectral PV absorption of a pure TFSC is close to perfect and cannot be noticeably enhanced. The integral absorption may be practically raised exploring the wavelength range of 400–500 nm. Really, in Fig. 3 we note a significant growth in this wavelength range granted by all our coatings. Unfortunately, for the flat ARC the increase of the spectral absorption at 400–475 nm obviously corresponds to a certain decrease of it in the range of 475–575 nm. This is why the enhancement is only 4.6%. The LTS offers better integral increase than the flat ARC over the whole range. The best result for the normal incidence corresponds to the LTS of tapered voids when the integral absorption attains 48%.

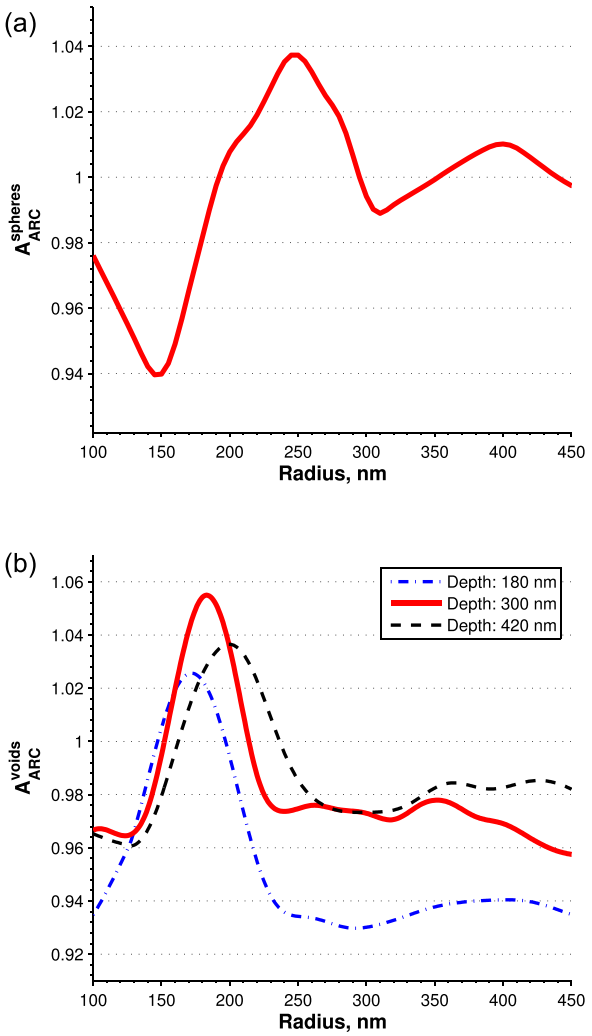

FIG. 2. (a) The ratio of the integral absorption at the presence of a layer of closely packed spheres (A_{spheres}) to the corresponding value A_{ARC} corresponding to an optimal flat ARC (fused silica glass). (b) The ratio of the integral absorption in the presence of a layer of tapered voids for several values of depth (A_{void}) to the corresponding value A_{ARC} for the optimal flat ARC. The taper angle and the minimal distance between adjacent voids are constant for all three cases and equal to 10° and 30 nm, respectively.

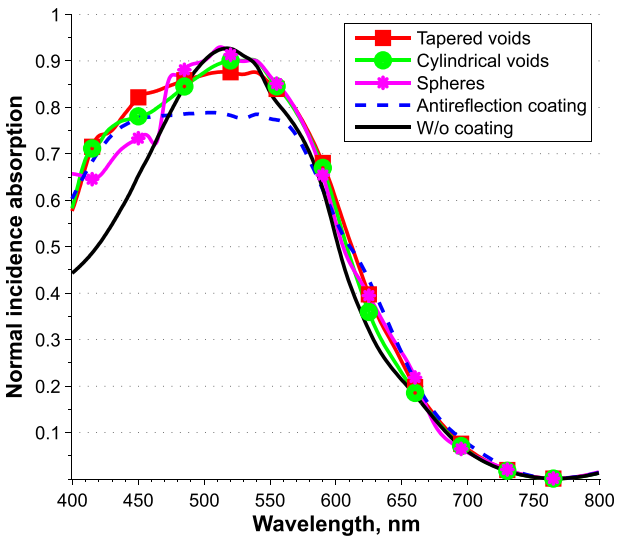

FIG. 3. Absorption spectra of the system for the following cases: pure TFSC (black solid line), flat ARC of fused silica glass (blue dashed line), layer of nanospheres (purple line), disk voids (green line), and tapered voids (of optimal radius and depth; red line).

B. Reflection suppression

Despite the quite similar effect over the wavelength spectrum, our nanostructures based on voids and spheres operate differently. To understand better this difference, we have studied separately how they affect the reflectance and transmittance.

Figure 4(a) shows dependencies of the reflectance from the TFSC on wavelength for all considered cases. It is obvious that the reflection is significantly lower when using ARC, spheres, or tapered voids than cylindrical nano-voids. Really, the relative integral reflection, compared to the reflection from pure surface

$$R_{\text{pure}}^{\text{struct.}} = \frac{\int R_{\text{struct.}}\, d\nu}{\int R_{\text{pure}}\, d\nu}, \tag{2}$$

where R_{pure}, $R_{\text{struct.}}$—reflection coefficients from pure surface and from TFSC with nano-structures, respectively, reaches the following values:

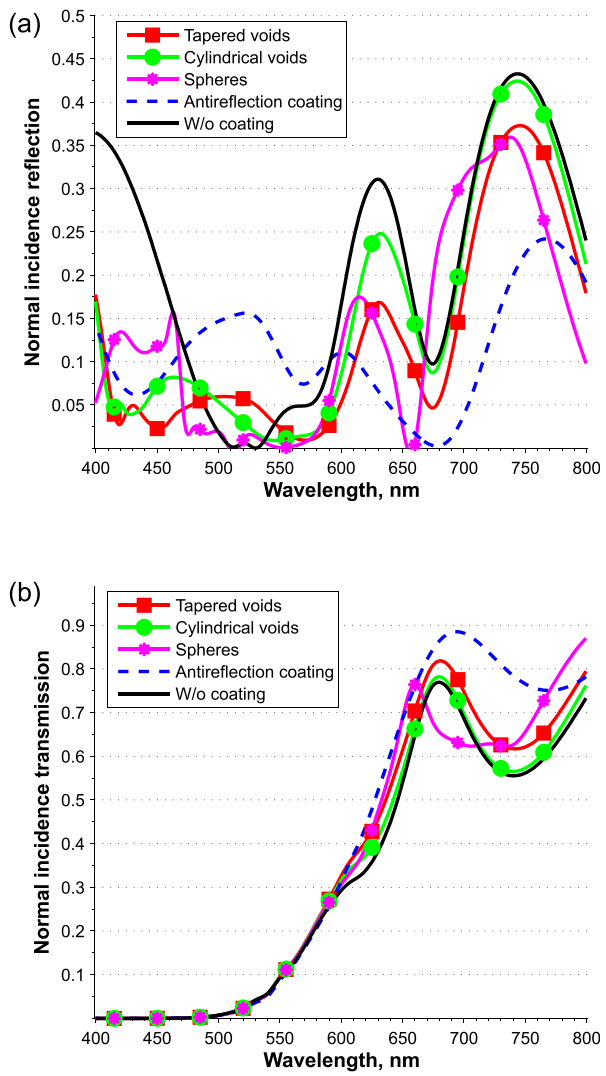

FIG. 4. Dependencies of the reflectance from the TFSC (a) and the transmittance through semiconductor layers (b) on wavelength for all considered cases.

(1) $R_{\text{pure}}^{\text{tapered voids}} = 0.607$.
(2) $R_{\text{pure}}^{\text{cylindrical voids}} = 0.748$.
(3) $R_{\text{pure}}^{\text{spheres}} = 0.643$.
(4) $R_{\text{pure}}^{\text{ARC}} = 0.539$.

The cylindrical nano-voids are noticeably worse than the array of nanospheres, tapered nano-voids or ARC, whereas the flat ARC offers the best suppression of reflection. Spheres emulate a textured layer. Both our previous research[29–32] and the results of other authors[28] show that the array of spheres can suppress the reflection better than ARC, but in fact such properties are strongly dependent on the solar cell design. Voids can be probably referred as the stepped effective refractive index profile.

Nevertheless, according to the results obtained in Sec. III A, our tapered nano-voids offer the integral absorption in the PV layer noticeably better than ARC. Therefore, light-trapping properties of arrayed voids should be studied.

C. Transmission suppression

Let us consider the energy transmitted through the PV-layers into the AZO substrate. As we have already mentioned, transmission losses are one of the most crucial problems for TFSC.

The dependencies of the part of energy transmitted into the substrate on wavelength are presented in Fig. 4(b). Optimal parameters for these structures were defined in Sec. III A.

It is not so simple to properly describe the reduction of the parasitic transmission through the PV layer in the presence of the reflection. In our case, the lowest integral transmittance T of the incident light to the AZO substrate corresponds to the pure (non-coated) TFSC. It is not surprising since the reflection from the open surface of the solar cell is, obviously, the highest one, and in spite of the rather low absorption only a small portion of the incident power transmits to AZO. The reduction of the reflectance results not only in the increase of the PV absorbance but also in the certain increase of T. Sometimes one introduces a coefficient defined as $T/(1-R)$ and the light-trapping implies the minimization of this coefficient. However, this coefficient is not very relevant when the PV absorption is close to the saturation, and the modification of the coating results in the rather slight enhancement of the integral A. In this situation, it is reasonable to insert the comparison with the pure TFSC into the coefficient describing the parasitic transmittance. We introduce a coefficient which describes the light-trapping efficiency (LTE) for different coating structures in comparison with the pure TFSC. This coefficient shows how the parasitic transmittance is modified by the presence of the structure

$$LTE_{\text{pure}}^{\text{struct.}} = \frac{R_{\text{pure}} - R_{\text{struct.}}}{T_{\text{struct.}} - T_{\text{pure}}}, \tag{3}$$

where $R(T)_{\text{pure}}$ and $R(T)_{\text{struct.}}$—integral reflection (transmission) coefficients of pure TFSC and TFSC with a coating structure, respectively. The minimal increase of the transmission together with a maximal decrease of reflection indicates

the best light-trapping property. This coefficient is significantly different for four coatings under study

(1) $LTE_{\text{pure}}^{\text{tapered voids}} = 2.57$.
(2) $LTE_{\text{pure}}^{\text{cylindrical voids}} = 5.04$.
(3) $LTE_{\text{pure}}^{\text{spheres}} = 2.54$.
(4) $LTE_{\text{pure}}^{\text{ARC}} = 1.31$.

The highest values of $LTE_{\text{pure}}^{\text{struct.}}$ coefficient are in the case of nano-voids. We can see that the cylindrical nano-voids possess better light-trapping properties than tapered nano-voids, though the last ones give the maximal gain in the PV absorption. The tapered voids are better than the cylindrical voids due to better antireflective properties. So, $LTE_{\text{pure}}^{\text{struct.}}$ is a relevant coefficient which stresses the suppression of the parasitic transmittance. Notice that the value of $LTE_{\text{pure}}^{\text{ARC}}$ is not unity, and it is not surprising. Obviously, a blooming layer suppresses the parasitic transmittance because it is reciprocally blooming and changes the balance between the energy transmitted to the AZO substrate and the energy reflected from the bottom interface (semiconductor-AZO) in favor of the last one.

To understand the advantage of the nano-voids compared to nano-spheres, let us consider the time-averaged distributions of the electric energy density in the structure. The corresponding color map is shown in Fig. 5. It can be seen that spheres transform an incident plane wave into collimated beams, as it was for a TFSC studied in Ref. 32. The parasitic absorption occurs in the top layer of AZO, and a rather attenuated beam transmits to the PV layer, resulting in the formation of a hot spot in the i-layer of a-Si. In the structure with nano-voids, multiple hot spots are formed over a unit cell. Besides a parasitic absorption in AZO, still several hot spots are formed in the i-layer of a-Si. Such multi-spot field distribution looks similar to that predicted for a metal nanoantennae array supporting domino-modes.[25–27] First, in both these structures hot spots are located mainly in between light-trapping inclusions (in the present case—voids).

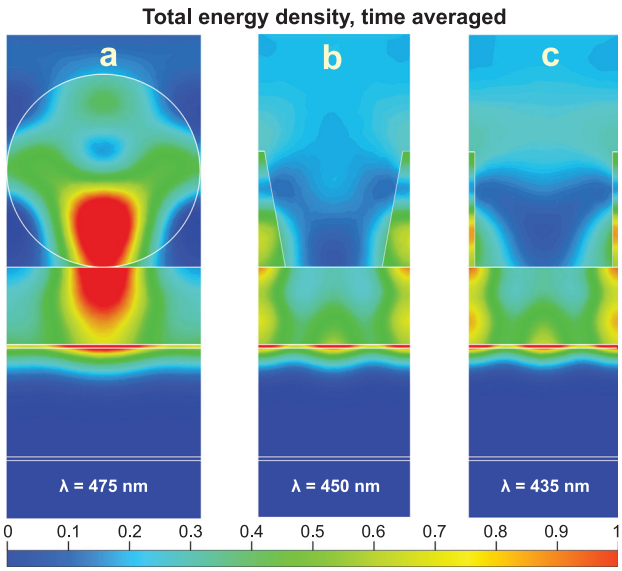

FIG. 5. The time-averaged distributions of the total energy density in the light-trapping structures under consideration.

Second, in both these structures the light-trapping regime is related to the mutual interaction of inclusions. Definitely, so optically small hot spots imply the excitation of evanescent waves. These waves are excited by the incident plane wave neither in a single void in the same structure nor in a sparse array of the same voids. The obtained effect is theoretically observed only for a specific unit cell dimensions. It is clearly seen comparing Fig. 5(a) to Figs. 5(b) and 5(c) that the hot spots in the case of nano-voids are much smaller. The smaller is the hot spot, the stronger is the absorption in it, and the light-trapping properties of nano-voids turn out to be better than those of nano-spheres.

IV. OBLIQUE INCIDENCE OF LIGHT

The dependence of the efficiency of a TFSC on the angle of incidence is one of the main characteristics since TFSC (unlike a wafer solar panel of a power station) does not rotate following the Sun. Thus, the study of the proposed LTS would not be complete without consideration of the stability of the PV absorption versus the incidence angle.

We studied the integral absorption enhancement for the optimal structures, whose parameters were found in Sec. III for the oblique incidence of light (0°–30°). The results are shown in Table I.

The PV absorption enhancement provided by the ARC is quite stable at these angles and only slightly decreases with increasing the angle up to 30° due to the red shift of the antireflection peak. In the case of nanospheres, the absorption rapidly decreases and the efficiency becomes higher than in the case of ARC only at small (<20°) angles for this solar cell design. Nevertheless, spheres show 3.7% efficiency enhancement in comparison with non-coated solar cell at the angle of 30°. Cylindrical voids show less dramatic decrease of the absorption comparing with spheres and exceed the efficiency granted by the ARC at angles of incidence up to 28°.

In the case of the tapered voids, integral absorption is substantially more stable to the angle of incidence and the absorption averaged over the angle is maximal for this case.

The total efficiency of all these structures can be described through the angular averaging of the integral absorption that corresponds to different positions of Sun. These values normalized to the case of the pure TFSC are as follows:

(1) $\langle A_{\text{pure}}^{\text{tapered voids}} \rangle = 1.087$.
(2) $\langle A_{\text{pure}}^{\text{cylindrical voids}} \rangle = 1.068$.
(3) $\langle A_{\text{pure}}^{\text{spheres}} \rangle = 1.058$.
(4) $\langle A_{\text{pure}}^{\text{ARC}} \rangle = 1.045$.

TABLE I. Values of the integral absorption (over the operating range of TFSC) at the presence of our LTS to the corresponding value A_{pure} for different angles of incidence of light.

Angle (deg)	$A_{\text{pure}}^{\text{tapered voids}}$	$A_{\text{pure}}^{\text{cylindrical voids}}$	$A_{\text{pure}}^{\text{spheres}}$	$A_{\text{pure}}^{\text{ARC}}$
0	1.105	1.088	1.085	1.046
10	1.096	1.082	1.062	1.046
20	1.075	1.06	1.046	1.045
30	1.07	1.042	1.037	1.044

Thus, the average gain over the angle has a maximum value for the LTS of tapered voids and is nearly equal 8.7%. This is a rather noticeable improvement for a quite substantial silicon TFSC with quite high initial PV absorption.

V. CONCLUSIONS

To summarize, we have studied three different all-dielectric structures offering an enhancement of the efficiency of the PV conversion in thin-film solar cells based on amorphous silicon. The suppression of both reflection and transmission was studied for the following systems:

(1) a flat anti-reflecting coating,
(2) an array of densely packed polystyrene nano-spheres,
(3) an array of nano-voids (cylindrical and tapered shape) in the PMMA layer.

The optimal parameters of the structures that provide the greatest absorption in the PV layer were found, and it was shown that three of our LTS offer the gain in the PV absorption which is more than the gain granted by the flat ARC. The anti-reflecting and light-trapping effects in our LTS are not resonant and fundamentally broadband. We found that the layer of cylindrical nano-voids has the highest light trapping efficiency. At the same time, tapered nano-voids allow to achieve highest integral absorption, because they reduce the reflection better than cylindrical ones. Therefore, tapered voids promise the best performance. The optimal structure grants the gain 8.7% over 0°–30° angles of incidence. Our slightly tapered voids can be fabricated using the nanoimprint lithography. The application of our LTS seems to be promising for TFSC of different configurations.

ACKNOWLEDGMENTS

This work has been partially supported by the Russian Fund for Basic Research (Grant No. 13-08-01438), (Grant No. 14-08-31730 mol_a), (Grant No. 14-02-31765 mol_a); the Government of the Russian Federation (Grant No. 074-U01); the Russian Ministry of Science and Education (Project No. 14.Z50.31.0015), (Project No. 11.G34.31.0020) and the Dynasty Foundation. A.S. acknowledges the support of the Ministry of Science and Education of the Russian Federation (GOSZADANIE 2014/190).

[1]A. Marti and A. Luque, *Next-Generation Photovoltaics* (Institute of Physics Publishing, Bristol, 2004).
[2]J. Nelson, *The Physics of Solar Cells* (Imperial College Press, 2003.
[3]M. A. Green, *Solar Cells: Operating Principles, Technology and System Applications* (University of South Wales, Sydney, 1998).
[4]See www.catharinafonds.nl/wp-content/uploads/2010/03/NanosolarCellWhitePaper.pdf for "Ultra-low-cost solar electricity cells," in An Overview of Nanosolars Cell Technology Platform, White paper (Nanosolar, Inc., 2009).
[5]Y. Yu, V. E. Ferry, A. P. Alivisatos, and L. Cao, Nano Lett. **12**, 3674–3681 (2012).
[6]P. Bermel, C. Luo, L. Zeng, L. C. Kimerling, and J. D. Joannopoulos, Opt. Express **15**, 16986 (2007).
[7]S. B. Mallick, M. Agrawal, and P. Peumans, Opt. Express **18**, 5691 (2010).
[8]P. Campbell and M. A. Green, J. Appl. Phys. **62**, 243 (1987).
[9]S. K. Rotich, J. G. Smith, A. G. R. Evans, and A. Brunnschweiler, J. Micromech. Microeng. **8**, 134–137 (1998).
[10]S. Pillai, K. R. Catchpole, T. Trupke, and M. A. Green, J. Appl. Phys. **101**, 093105 (2007).
[11]N. C. Panoiu and R. M. Osgood, Opt. Lett. **32**, 2825–2829 (2007).
[12]K. R. Catchpole and A. Polman, Appl. Phys. Lett. **93**, 191113 (2008).
[13]Yu. A. Akimov, K. Ostrikov, and E. P. Li, Plasmonics **4**, 107 (2009).
[14]C. Rockstuhl and F. Lederer, Appl. Phys. Lett. **94**, 213102 (2009).
[15]M. E. Ferry, L. A. Sweatlock, D. Pacifici, and H. A. Atwater, Nano Lett. **8**, 4391–4397 (2008).
[16]R. A. Pala, J. White, E. Barnard, J. Liu, and M. L. Brongersma, Adv. Mater. **21**, 3504–3509 (2009).
[17]P. A. Spinelli, V. E. Ferry, J. van de Groep, M. van Lare, M. A. Verschuuren, R. E. I. Schropp, H. A. Atwater, and A. Polman, J. Opt. **14**, 024002 (2012).
[18]Y. Wang, T. Sun, T. Paudel, Y. Zhang, Zh. Ren, and K. Kempa, Nano Lett. **12**, 440–443 (2012).
[19]H. A. Atwater and A. Polman, Nature Mater. **9**, 205–208 (2010).
[20]E. Yablonovitch and G. D. Cod, IEEE Trans. Electron. Devices **29**, 300 (1982).
[21]D. M. Callahan, J. N. Munday, and H. A. Atwater, Nano Lett. **12**, 214–218 (2012).
[22]V. M. Agranovich and D. L. Mills, *Surface Polaritons - Electromagnetic Waves at Surfaces and Interfaces* (Elsevier Science Ltd, Amsterdam, 1982).
[23]Z. Yu, A. Raman, and S. Fan, Opt. Express **18**, A366–A380 (2010).
[24]J. Grandidier, D. M. Callahan, J. N. Munday, and H. A. Atwater, Adv. Mater. **23**, 1272–1276 (2011).
[25]C. Simovski, D. Morits, P. Voroshilov, M. Guzhva, P. Belov, and Yu. Kivshar, Opt. Express **21**, A714–A725 (2013).
[26]P. M. Voroshilov, C. R. Simovski, and P. A. Belov, J. Mod. Opt. **61**, 1743–1748 (2014).
[27]I. S. Sinev, P. M. Voroshilov, I. S. Mukhin, A. I. Denisyuk, M. E. Guzhva, A. K. Samusev, P. A. Belov, and C. R. Simovski, Nanoscale **7**, 765–770 (2015).
[28]T. H. Chang, P. H. Wu, S. H. Chen, C. H. Chan, C. C. Lee, C. C. Chen, and Ya. K. Su, Opt. Express **17**, 6519–6524 (2009).
[29]A. S. Shalin, JETP Lett. **91**, 636–642 (2010).
[30]A. S. Shalin, Quantum Electron. **41**, 163 (2011).
[31]A. S. Shalin, Prog. Electromagn. Res. B **31**, 45–66 (2011).
[32]C. R. Simovski, A. S. Shalin, P. M. Voroshilov, and P. A. Belov, J. Appl. Phys. **114**, 103104 (2013).
[33]A. Luke and S. Hegedus, *Handbook of Photovoltaic Science and Engineering* (Wiley, Chichester, UK, 2002), p. 518.
[34]A. S. Ferlauto, G. M. Ferreira, J. M. Pearce, C. R. Wronski, R. W. Collins, X. Deng, and G. Ganguly, J. Appl. Phys. **92**, 2424 (2002).
[35]G. V. Naik, J. Kim, and A. Boltasseva, Opt. Mater. Express **1**, 1090 (2011).
[36]S. N. Kasarova, N. G. Sultanova, C. D. Ivanov, and I. D. Nikolov, Opt. Mater. **29**, 1481–1490 (2007).
[37]M. I. Mishchenko, L. D. Travis, and A. A. Lacis, *Scattering, Absorption, and Emission of Light by Small Particles* (Cambridge University Press, 2002).
[38]F. Lasnier and T. G. Ang, *Photovoltaic Engineering Handbook* (Adam Hilger, Bristol, UK, 1990), p. 209.
[39]R. Kitamura, L. Pilon, and M. Jonasz, Appl. Opt. **46**, 8118–8133 (2007).